Geophys. J. R. astr. Soc. (1975) **43**, 795–814

The Effect of Anelasticity on Periods of the Earth's Free Oscillations (Toroidal Modes)*

Hsi-Ping Liu and Charles B. Archambeau

(Received 1975 May 6)†

Summary

It is known that the anelastic properties of the Earth characterized by a 'Q' structure will affect the periods of free oscillation. It is generally considered that the effect is negligible compared to the other perturbing effects due to rotation, ellipticity, and lateral inhomogeneities. Nevertheless, it is of some interest to investigate the precise magnitude of this effect for the observed free oscillation modes since it could provide us with another constraint in the determination of the Q structure of the Earth. An application of perturbation theory provides us with a good estimate of the magnitude of the changes in the periods of an elastic model due to inclusion of anelastic effects. Calculations based on currently accepted mean elastic and anelastic models for the Earth show that the shift in period due to anelasticity is at most 0·023 per cent for the toroidal modes from ${}_0T_2$ to ${}_0T_{99}$, the maximum occurring near ${}_0T_{60}$. For more extreme Q models, which may be locally applicable, period shifts of the order 0·1 per cent occur, with the maximum again near ${}_0T_{60}$, corresponding to a period of approximately 150 s. Observational accuracy for the toroidal oscillations is around 0·1 per cent so that anelastic shifts in toroidal oscillation periods are at the present limit of observational accuracy. Viewed in terms of propagating surface waves, the dispersion due to anelasticity results in at most 0·005–0·01 km s^{-1} variations in the phase and group velocities. Such shifts are within the observational resolution of surface dispersion measurements using narrow band filtering techniques. Compared to other perturbing effects, anelasticity is significant for the toroidal oscillation only in the 50- to 300-s period range. In this range, lateral variations in structure generally cause larger perturbations. However, when viewed in terms of propagating surface waves in selected homogeneous regions, anelasticity becomes the dominating effect. Further, the frequency shift due to anelasticity is scaled by $(1/Q)^2$, so that the anelastic effect can be well within observational accuracy and comparable to any perturbing effect for more extreme, yet acceptable, Q models. In particular, when applied to surface waves propagating across a tectonic region with a strong low velocity zone in the upper mantle, the anelasticity induced dispersion on frequency shift can be significant and measurable. In such cases a joint inversion of elastic and anelastic properties is appropriate.

• California Institute of Technology Contribution No. 2575.

† Received in original form 1975 February 28

1. Introduction

The anelasticity of the Earth's interior gives rise to a variety of important phenomena in solid earth geophysics. Examples are the short-period effects such as seismic wave attenuation and tidal dissipation; the long-term phenomena such as response of Earth's crust and mantle to loading and unloading on the surface ('isostasy') or the transverse movements of large segments of Earth's upper layers ('plate tectonics'). The mechanisms responsible for the anelastic behaviour of the Earth's interior are largely controlled by defect structure of the crystals making up the rock minerals. A host of such mechanisms, thought to be applicable to geophysics, are reviewed and listed in the literature (Gordon & Nelson 1966; Jackson & Anderson 1970). Further experimentation under high pressure and temperature pertinent to mantle conditions are necessary to decide their relative importance.

Recently, the attenuation of seismic body and surface waves at different frequencies have been measured. Jackson & Anderson (1970) summarize this information up to 1970. This information, when carefully interpreted, can serve to put a constraint on the physical mechanisms of anelasticity operating in the Earth's interior.

It is the purpose of the present work to determine whether anelasticity, as inferred from the seismic wave attenuation data, also produces a non-negligible shift in the periods of Earth's toroidal oscillations. Here the idea is to see whether we can use both the amplitude data and the frequency shifts to infer the anelastic properties of the Earth. If the frequency shifts due to anelasticity are large enough to be measured, then a joint inversion for elastic and anelastic properties of the Earth could be attempted. We anticipate that the frequency shifts due to anelasticity will be small. However, two considerations below lead us to try to obtain precise theoretical estimates. (1) The precision of free oscillation period determinations has steadily improved and has reached a level suggesting that, at least at some frequencies, the effect of anelasticity may be resolved. (2) The current anelastic models for the Earth are based on an average of the Earth as a whole so that quite extreme variations of the anelastic properties could be expected within some tectonic provinces. Much larger effects than would be inferred from mean earth anelastic models would therefore be reflected in 'local' measurements or in short wave length measurements in the surface wave frequency range. With respect to the first of these, Dziewonski & Gilbert (1972) recently determined the free oscillation periods excited by the 1964 Alaskan earthquake. The resolution of the fundamental toroidal modes ${}_0T_l$ reported by them varies between 0·031 and 0·262 per cent and is generally about 0·1 per cent for the higher frequency toroidal modes ${}_0T_l$ at which the anelastic shift becomes important. Hence we will consider predicted fractional shifts in the free oscillation periods of the order of $|\Delta T/T| \sim 10^{-3}$ to be significant and measurable effects. We will consider a variety of anelastic models, using both the constant intrinsic Q models and particular frequency dependent Q models, covering a range of possibilities that appear to us to be reasonable for the Earth, both for its mean anelastic properties and for the anelastic properties likely to occur in particular regions of the Earth's interior. We will compute both the amplitude effects to be observed (i.e. the amplitude decrement of the free oscillations or the line width of the free oscillation power spectrum) and the centre frequency shifts by means of a perturbation theory. In this case the frequency shift is obtained from the second-order perturbation calculation while the line width or amplitude decrement is obtained from the first-order perturbation result. The amplitude decrement based on a perturbation calculation was previously obtained by Anderson & Archambeau (1964). Since the calculation is a perturbation result, the effects are expressed relative to an unperturbed, ideally elastic Earth model. The results of the amplitude decrement will be compared to the available observations for each of the anelastic models used in the calculation, while the associated frequency shifts will be compared to the resolution limit of 0·1 per cent and to the magnitudes

of other perturbing effects such as ellipticity and lateral inhomogeneity in order to assess the importance and measurability of the anelastic effect.

2. Perturbation calculation of the shift in the Earth's toroidal oscillation periods due to anelasticity

The equation of motion for the elastic-gravitational oscillation of a non-rotating earth with lateral heterogeneity is given by

$$\rho_0(\omega_{kl}^m)^2\,\mathbf{S}_{kl}^m = H(\mathbf{S}_{kl}^m, \phi) \tag{1}$$

and

$$\nabla^2\phi_1 = 4\pi G\nabla.(\rho_0\,\mathbf{S}_{kl}^m) \tag{2}$$

where

ρ_0 : equilibrium density distribution

$\mathbf{S}_{kl}^m$: displacement field of free oscillation characterized by the mode numbers k, l and m

ω_{kl}^m : angular oscillation frequency

$\rho_1 = -\nabla.(\rho_0\,\mathbf{S}_{kl}^m)$, change in density due to displacement

$\phi = \phi_0+\phi_1$, total gravitational potential

ϕ_0 : equilibrium gravitational potential

ϕ_1 : change in gravitational potential due to free oscillation

G : gravitational constant.

The operator H is defined by its components in Cartesian co-ordinates (Dahlen 1968) by

$$\begin{aligned}[H(\mathbf{S},\phi)]_i = {} & -\partial_j(\Gamma_{ijkl}\,\sigma_{kl})+\partial_i[\rho_0\,S_j\,\partial_j\phi_0]-\nabla.(\rho_0\,\mathbf{S})\partial_i\phi_0\\ & +\rho_0\,\partial_i\phi_1-\partial_i[S_k\,\partial_j\,\tau_{kj}{}^0]+\partial_j(S_k\,\partial_k\,\tau_{ij}{}^0]\\ & +\partial_j[\tfrac{1}{2}\tau_{jl}{}^0(\partial_i\,S_l-\partial_l\,S_i)]+\partial_j[\tfrac{1}{2}\tau_{il}{}^0(\partial_j\,S_l-\partial_l\,S_j)]\end{aligned} \tag{3}$$

The mode numbers are suppressed in the above equation. In equation (3) where

$\sigma_{kl} \equiv (\partial_k\,S_l+\partial_l\,S_k)/2$

$\mathbf{T}^0$: static stress field tensor

$\boldsymbol{\tau}^0 \equiv \mathbf{T}_0-\frac{1}{3}(\mathbf{T}_0)_{ii}\,\mathbf{I}$, is the static stress deviator tensor

$\mathbf{E}$: elastic stress tensor

and the stress-strain relationship (in Cartesian co-ordinates)

$$E_{ij} = \Gamma_{ijkl}\,\sigma_{kl}-\tfrac{1}{2}\tau_{jl}{}^0(\partial_i\,S_l-\partial_l\,S_i)-\tfrac{1}{2}\tau_{il}{}^0(\partial_j\,S_l-\partial_l\,S_j) \tag{4}$$

has been used in the equation of motion to obtain the expression for operator $H(\mathbf{S}, \phi)$ in equation (3). Γ_{ijkl} in equation (4) are components of the elastic coefficient tensor. The boundary conditions are (Alterman, Jarosch & Pekeris 1959; Backus 1967)

$$\left.\begin{array}{l}\mathbf{S} \text{ continuous, except at mantle–core boundary where only } \hat{\mathbf{n}}.\mathbf{S} \text{ needs to be continuous}\\ \phi_1 \text{ continuous}\\ \hat{\mathbf{n}}.\nabla\phi_1+\mathbf{S}.\hat{\mathbf{n}}4\pi G\rho_0 \text{ continuous}\\ \hat{\mathbf{n}}.\mathbf{E} \text{ continuous}\end{array}\right\} \tag{5}$$

where $\hat{\mathbf{n}}$ is the outward normal to an undeformed surface of continuity.

Equation (2) can be integrated to express $\phi_1(\mathbf{r})$ in terms of the displacement field $\mathbf{S}$

$$\phi_1(\mathbf{r}) = -G\int \nabla.(\rho_0 \mathbf{S})g(\mathbf{r},\mathbf{r}')dV' + G\int \rho_0(\mathbf{r}')g(\mathbf{r},\mathbf{r}')S(\mathbf{r}').\hat{\mathbf{n}}'dS' \tag{6}$$

$$g(\mathbf{r},\mathbf{r}') = 1/|\mathbf{r}-\mathbf{r}'|$$

The eigenvalue equation of the adjoint operator, $\tilde{H}$, is

$$\tilde{H}(\tilde{\mathbf{S}}_{kl}^{m}) = (\gamma_{kl}^{m})^2 \rho_0 \tilde{\mathbf{S}}_{kl}^{m} \tag{7}$$

with

$$\int \rho_0 \tilde{\mathbf{S}}_{kl}^{m}.\mathbf{S}_{k'l'}^{m'}\,dV = 0 \quad \text{if} \quad k \neq k', \quad l \neq l' \quad \text{or} \quad m \neq m'$$

$\tilde{\mathbf{S}}_{kl}^{m}$ is the adjoint solution of $\mathbf{S}_{kl}^{m}$. If H is hermitian, $\tilde{H} = H$, $\gamma_{kl}^{m} = \omega_{kl}^{m}$ and $\tilde{\mathbf{S}}_{kl}^{m} = \bar{\mathbf{S}}_{k}^{m}$, where $\bar{\mathbf{S}}_{kl}^{m}$ denotes complex conjugate of $\mathbf{S}_{kl}^{m}$. In the present problem for toroidal oscillations, the operator H is hermitian. We will nevertheless employ the adjoint notation in the perturbation calculation until the end and then taking note of the fact that H is hermitian.

The straightforward way of introducing anelasticity into the equation of motion is to assume a constitutive relation which contains dissipation factors. The simplest such constitutive relation results from introducing complex moduli of elasticity into the linear stress-strain relation as expressed by equation (4). As an illustration, consider the stress-strain relation of a visco-elastic solid,

$$E_{ij} = \lambda\sigma_{ii}\delta_{ij} + 2\mu\sigma_{ij} + \lambda'\frac{\partial\sigma_{ii}}{\partial t}\delta_{ij} + 2\mu'\frac{\partial\sigma_{ij}}{\partial t} \tag{8}$$

where λ, λ', μ, μ' are real quantities. In the frequency domain (or in response to sinusoidal disturbance) the stress-strain relation (8) takes the form

$$E_{ij} = (\lambda + i\omega\lambda')\sigma_{ii}\delta_{ij} + 2(\mu + i\omega\mu')\sigma_{ij} \tag{9}$$

which shows that a pure imaginary part in the elastic moduli would account for this specific anelastic behaviour. Further, a wider class of anelastic behaviour can be represented in this manner as noted, for example, by Anderson & Archambeau (1964). In an anisotropic medium, the more general equation corresponding to equation (9) is

$$[\mathscr{H}(\mathbf{S})]_i = -\partial_j(\Gamma^{*}_{ijkl}\,\sigma_{kl}) \tag{10}$$

where Γ^{*}_{ijkl} is a tensor with complex components and having the same form as the elastic tensor Γ_{ijkl}. In an isotropic material, the operator $\mathscr{H}$ takes the form

$$\mathscr{H}\mathbf{S} = -(\lambda^*+2\mu^*)\nabla(\nabla.\underset{\sim}{\ }) + \mu^*(\nabla\times(\nabla\times\underset{\sim}{\ })) - (\nabla\lambda^*)(\nabla\underset{\sim}{\ }) - (\nabla\mu^*).(\nabla\underset{\sim}{\ } + \underset{\sim}{\ }\nabla) = [H+A]\mathbf{S} \tag{11}$$

where

$$(\nabla\mathbf{S}+\mathbf{S}\nabla)/2 = \mathbf{i}e_{11}\mathbf{i} + \mathbf{j}e_{22}\mathbf{j} + \mathbf{k}e_{33}\mathbf{k} + e_{12}(\mathbf{ij}+\mathbf{ji}) + e_{13}(\mathbf{ik}+\mathbf{ki}) + e_{23}(\mathbf{jk}+\mathbf{kj})$$

in the dyadic notation, with $e_{ij} = \frac{1}{2}(\partial_i S_j + \partial_j S_i)$. Here H is the real part and A the imaginary part of the operator $\mathscr{H}$. With the anelastic operator A, the eigenvalue equation describing the Earth's free oscillations becomes

$$H(\mathbf{S}_{kl}^{m}) + A(\mathbf{S}_{kl}^{m}) = \rho_0(\omega_{kl}^{m})^2\,\mathbf{S}_{kl}^{m}. \tag{12}$$

We will restrict the treatment to an isotropic stress-strain relation and consider the anelastic behaviour as a perturbation. The perturbation expansion for the angular frequency and the displacement field are

$$\left.\begin{aligned} \omega_{kl}^{m} &= \omega_{kl}^{(0)m} + \omega_{kl}^{(1)m} + \omega_{kl}^{(2)m} + \dots \\ \gamma_{kl}^{m} &= \gamma_{kl}^{(0)m} + \gamma_{kl}^{(1)m} + \gamma_{kl}^{(2)m} + \dots \\ \mathbf{S}_{kl}^{m} &= \mathbf{S}_{kl}^{(0)m} + \mathbf{S}_{kl}^{(1)m} + \mathbf{S}_{kl}^{(2)m} + \dots \end{aligned}\right\} \tag{13}$$

Substituting equation (13) into equation (12), the zeroth order equation is

$$H(\mathbf{S}_{kl}^{(0)m}) = \rho_0(\omega_{kl}^{(0)m})^2\,\mathbf{S}_{kl}^{(0)m} \tag{14}$$

i.e. the elasto-gravitational oscillation of a non-rotating Earth. The first order equation is

$$H(\mathbf{S}_{kl}^{(1)m}) + A(\mathbf{S}_{kl}^{(0)m}) = \rho_0(\omega_{kl}^{(0)m})^2\,\mathbf{S}_{kl}^{(1)m} + 2\omega_{kl}^{(1)m}\,\omega_{kl}^{(0)m}\,\rho_0\,\mathbf{S}_{kl}^{(0)m} \tag{15}$$

$\mathbf{S}_{kl}^{(1)m}$ can be expanded in terms of the zeroth order eigenfunctions as

$$\mathbf{S}_{kl}^{(1)m} = \sum_{m'\neq m} a_{mm'}^{(1)}\,\mathbf{S}_{kl}^{(0)m'} + \sum_{k'\neq k} b_{kk'}^{(1)}\,\mathbf{S}_{k'l}^{(0)m} + \sum_{l'\neq l} c_{ll'}^{(1)}\,\mathbf{S}_{kl'}^{(0)m} \tag{16}$$

Now taking the dot product of equation (15) with $\tilde{\mathbf{S}}_{kl}^{(0)m}$, the adjoint solution of $\mathbf{S}_{kl}^{(0)m}$, and integrating over the volume. We have, by definition of the adjoint solution,

$$\int \tilde{\mathbf{S}}_{kl}^{(0)m}.\,H(\mathbf{S}_{kl}^{(1)m})dV = \int \mathbf{S}_{kl}^{(1)m}.\tilde{H}(\tilde{\mathbf{S}}_{kl}^{(0)m})dV \tag{17}$$

and equation (7), the first-order equation reduces to

$$\omega_{kl}^{(1)m} = \int \tilde{\mathbf{S}}_{kl}^{(0)m}.A\mathbf{S}_{kl}^{(0)m}\,dV/(2\omega_{kl}^{(0)m}\int \rho_0\,\tilde{\mathbf{S}}_{kl}^{(0)m}.\mathbf{S}_{kl}^{(0)m}dV) \tag{18}$$

Taking the dot product of equation (15) with $\tilde{\mathbf{S}}_{kl}^{(0)m'}$, $m' \neq m$, and noting that

$$\int \tilde{\mathbf{S}}_{kl}^{(0)m'}.\,H(\mathbf{S}_{kl}^{(1)m})dV = \int \mathbf{S}_{kl}^{(1)m}.\tilde{H}(\tilde{\mathbf{S}}_{kl}^{(0)m'})dV = \int \rho_0(\gamma_{kl}^{(0)m'})^2\,\mathbf{S}_{kl}^{(1)m}.\tilde{\mathbf{S}}_{kl}^{(0)m'}\,dV \tag{19}$$

equation (15) becomes

$$[(\gamma_{kl}^{(0)m'})^2 - (\omega_{kl}^{(0)m})^2]\int \rho_0\,\mathbf{S}_{kl}^{(1)m}.\tilde{\mathbf{S}}_{kl}^{(0)m'}\,dV = -\int \tilde{\mathbf{S}}_{kl}^{(0)m'}.A(\tilde{\mathbf{S}}_{kl}^{(0)m})dV \tag{20}$$

Substituting equation (16) into equation (20) gives

$$a_{mm'} = \int \tilde{\mathbf{S}}_{kl}^{(0)m'}.A(\mathbf{S}_{kl}^{(0)m})dV/\{[(\omega_{kl}^{(0)m})^2 - \gamma(_{kl}^{(0)m'})^2]\times\int\rho_0\tilde{\mathbf{S}}_{kl}^{(0)m'}.\mathbf{S}_{kl}^{(0)m'}dV\} \tag{21}$$

Similarly, expressions for $b_{kk'}$ and $c_{ll'}$ are obtained by taking dot products of equations with $\tilde{\mathbf{S}}_{k'l}^{(0)m}$ and $\tilde{\mathbf{S}}_{kl'}^{(0)m}$ respectively and integrating the resulting equation over the entire volume of the Earth. Now the second-order perturbation is

$$\begin{aligned} H(\mathbf{S}_{kl}^{(2)m}) + A(\mathbf{S}_{kl}^{(1)m}) = {} & \rho_0[(\omega_{kl}^{(1)m})^2 + 2\omega_{kl}^{(0)m}\,\omega_{kl}^{(2)m}]\mathbf{S}_{kl}^{(0)m} \\ & + \rho_0(\omega_{kl}^{(0)m})^2\,\mathbf{S}_{kl}^{(2)m} + 2\rho_0\,\omega_{kl}^{(0)m}\,\omega_{kl}^{(1)m}\,\mathbf{S}_{kl}^{(1)m}. \end{aligned} \tag{22}$$

Taking the dot product of equation (22) with $\tilde{\mathbf{S}}_{kl}^{(0)m}$ and integrating over the entire volume, with

$$\int \tilde{\mathbf{S}}_{kl}^{(0)m}.H(\mathbf{S}_{kl}^{(2)m})dV = \int \mathbf{S}_{kl}^{(2)m}.\tilde{H}(\tilde{\mathbf{S}}_{kl}^{(0)m})dV = \int \rho_0(\gamma_{kl}^{(0)m})^2\,\mathbf{S}_{kl}^{(2)m}.\tilde{\mathbf{S}}_{kl}^{(0)m}\,dV \tag{23}$$

equation (22) becomes

$$\begin{aligned} & \int \tilde{\mathbf{S}}_{kl}^{(0)m}.A(\mathbf{S}_{kl}^{(1)m})dV + [(\gamma_{kl}^{(0)m})^2 - (\omega_{kl}^{(0)m})^2].\int \rho_0\,\mathbf{S}_{kl}^{(2)m}.\tilde{\mathbf{S}}_{kl}^{(0)m}\,dV \\ & \qquad = [(\omega_{kl}^{(1)m})^2 + 2\omega_{kl}^{(0)m}\,\omega_{kl}^{(2)m}]\int \rho_0\,\tilde{\mathbf{S}}_{kl}^{(0)m}.\mathbf{S}_{kl}^{(0)m}\,dV \end{aligned} \tag{24}$$

or

$$\omega_{kl}^{(2)m} = \frac{\{\int \tilde{\mathbf{S}}_{kl}^{(0)m}.A(\mathbf{S}_{kl}^{(1)m})dV + [(\gamma_{kl}^{(0)m})^2 - (\omega_{kl}^{(0)m})^2]\int \rho_0\,\mathbf{S}_{kl}^{(2)m}.\tilde{\mathbf{S}}_{kl}^{(0)m}\,dV\}}{2\omega_{kl}^{(0)m}\int \rho_0\,\tilde{\mathbf{S}}_{kl}^{(0)m}.\mathbf{S}_{kl}^{(0)m}\,dV} - \tfrac{1}{2}(\omega_{kl}^{(1)m})^2/\omega_{kl}^{(0)m}. \tag{25}$$

This general result can now be applied to the toroidal oscillations of the Earth. The displacement field of an elastically isotropic and laterally homogeneous Earth model is taken as the zeroth order unperturbed eigenfunction. The operator H associated

with such an Earth model is hermitian. Therefore, $\tilde{H} = H$, $\tilde{\mathbf{S}}_{kl}{}^{m} = \bar{\mathbf{S}}_{kl}^{m}$, and $\gamma_{kl}{}^{m} = \omega_{kl}{}^{m}$. The zeroth order displacement field is then (e.g. Alterman *et al.* 1959).

$$\mathbf{S}_{kl}{}^{(0)m} = \mathbf{C}_l^m(\theta, \phi) W_{kl}(r) \tag{26}$$

where $\mathbf{C}_l^m(\theta, \phi)$ is the vector spherical harmonic defined by

$$\mathbf{C}_l^m(\theta, \phi) = \left(\hat{\mathbf{e}}_\theta \frac{\partial}{\partial\theta} + \hat{\mathbf{e}}_\phi \frac{\partial}{\partial\phi} \frac{1}{\sin\theta}\right) \times (\hat{\mathbf{e}}_r\, Y_l^m(\theta, \phi)) \tag{27}$$

$\hat{\mathbf{e}}_r$, $\hat{\mathbf{e}}_\theta$, $\hat{\mathbf{e}}_\phi$ are unit vectors in spherical polar co-ordinates, and

$$Y_l^m(\theta, \phi) = (-)^m \left[\frac{(2l+1)}{4\pi} \frac{(l-m)!}{(l+m)!}\right]^{\frac{1}{2}} P_l^m(\cos\theta) e^{im\phi}$$

is the spherical harmonic function. $W_{kl}(r)$ is solution to the equation

$$\mu_s^{(0)} \left[\frac{1}{r^2} \frac{d}{dr}\left(r^2 \frac{d}{dr}\right) - \frac{l(l+1)}{r^2}\right] W_{kl}(r) + \rho_s^{(0)} (\omega_{kl}{}^{(0)})^2 W_{kl}(r) = 0 \tag{28}$$

for a layered Earth model where $\mu_s^{(0)}$ and $\rho_s^{(0)}$ are rigidity and density inside the layer of index s, $s = 1, 2, \ldots, N$. The boundary conditions for equation (28) are continuity of $W_{kl}(r)$ and $(\mu^{(0)} d/(dr) W_{kl}(r) - W_{kl}(r))$ at layer boundaries. The adjoint displacement field is given by

$$\tilde{\mathbf{S}}_{kl}{}^{(0)m} = \bar{\mathbf{C}}_l^m(\theta, \phi) W_{kl}(r). \tag{29}$$

Assuming a laterally homogeneous anelasticy in the Earth model, with $\mu^{\updownarrow} = \mu^{(0)} + i\mu^{(1)}$

$$\left.\begin{aligned} &\int \tilde{\mathbf{S}}_{kl}{}^{(0)m} . A(S_{kl}{}^{(0)m}) dV = (\omega_{kl}{}^{(0)})^2 \int \frac{i\mu^{(1)}}{\mu^{(0)}} \rho^{(0)} W_{kl}(r) W_{kl}(r) dV \\ \text{and} \\ &(\omega_{kl}{}^{(0)}) \int \rho^{(0)} \tilde{\mathbf{S}}_{kl}{}^{(0)m} . \mathbf{S}_{kl}{}^{(0)m} dV = (\omega_{kl}{}^{(0)}) \int \rho^{(0)} [W_{kl}(r)]^2 dV. \end{aligned}\right\} \tag{30}$$

Substituting equation (30) into equations (18), (21) and (25) we get

$$\omega_{kl}{}^{(1)m} = \frac{\left\{\int \frac{i\mu^{(1)}}{\mu^{(0)}} \rho^{(0)} [W_{kl}(r)]^2 dV\right\} \omega_{kl}{}^{(0)}}{2 \int \rho^{(0)} [W_{kl}(r)]^2 dV} \equiv \tfrac{1}{2} \gamma_{kl}{}^{(1)} (\omega_{kl}{}^{(0)}) \tag{31}$$

and

$$\begin{aligned} \omega_{kl}{}^{(2)m} &= (\omega_{kl}{}^{(0)}) \left\{ \tfrac{1}{2} \sum_{i \neq k} \frac{\left| \int \frac{\mu^{(1)}}{\mu^{(0)}} W_{il}(r) W_{kl}(r) \rho^{(0)} dV \right|^2}{(\int \rho^{(0)} [W_{il}(r)]^2 dV)(\int \rho^{(0)} [W_{kl}(r)]^2 dV)} \right. \\ &\quad \left. \times \frac{(\omega_{il}{}^{(0)})^2}{(\omega_{il}{}^{(0)})^2 - (\omega_{kl}{}^{(0)})^2} + \frac{1}{2(\omega_{kl}{}^{(0)})^2} (\omega_{kl}{}^{(1)m})^2 \right\} \\ &\equiv (\omega_{kl}{}^{(0)}) \left\{ \frac{\gamma_{kl}{}^{(2)}}{2} + \frac{1}{2} \left(\frac{\gamma_{kl}{}^{(1)}}{2}\right)^2 \right\}. \end{aligned} \tag{32}$$

The attenuation factor (Q_{kl}^m) of the toroidal oscillation is given by

$$(Q_{kl}^m)^{-1} = 2\,\mathrm{Im}\left(\frac{\omega_{kl}^{(1)m}}{\omega_{kl}^{(0)m}}\right) = \gamma_{kl}^{(1)} \tag{33}$$

and the frequency shift is given by $\omega_{kl}^{(2)m}$.

3. Numerical calculations and results

In actual computation, a laterally homogeneous Earth model consisting of seismic velocities V_p, V_s and density $\rho^{(0)}$ as a function of radius is used in a normal mode program to generate the displacement function $W_{kl}(r)$ and angular frequency $\omega_{kl}^{(0)}$ for ${}_kT_l$, $k = 0, 1$; $l = 2, 3, \ldots, 99$. (m is degenerate for a laterally homogeneous, non-rotating, spherical Earth model). These, together with an intrinsic Q-model as a function of radius, are used to compute the free oscillation dissipation factor $(Q_{k=0,\,l})^{-1}$ and the frequency shift due to anelasticity $\omega^2_{k=0,l}$. Equations (31), (32) and (33) are employed in these computations. Note from equation (32)

$$\gamma^{(2)}_{k=0,l} = \sum_{i=1}^{\infty} \frac{\left|\int \frac{\mu^{(1)}}{\mu^{(0)}} W_{il}(r) W_{k=0,\,l}(r)\rho^{(0)} dV\right|^2}{\left[\int \rho^{(0)}[W_{il}(r)]^2\,dV\right]\left[\int \rho^{(0)}[W_{k=0,\,l}(r)]^2\,dV\right]} \cdot \frac{(\omega_{il}^{(0)})^2}{(\omega_{il}^{(0)})^2 - (\omega^{(2)}_{k=0,l})^2} \tag{34}$$

So that $\gamma^{(2)}_{k=0,l}$ is a summation of positive terms. Since

$$\omega_{il}^{(0)} > \omega^{(0)}_{k=0,l} \qquad i = 1, 2, \ldots \tag{35}$$

the computed value arising from the first term of the series:

$$_{i=1}\gamma^{(2)}_{k=0,l} = \frac{\left|\int \frac{\mu^{(1)}}{\mu^{(0)}} \rho^{(0)} W_{k=1,\,l}(r) W_{k=0,\,l}\,dV\right|^2}{\left(\int \rho^{(0)}[W_{k=1,\,l}(r)]^2\,dV\right)\left(\int \rho^{(0)}[W_{k=0,\,l}(r)]^2\,dV\right)}$$

$$\times \frac{(\omega^{(0)}_{k=1,l})^2}{(\omega^{(0)}_{k=1,l})^2 - (\omega^{(0)}_{k=0,l})^2} \tag{36}$$

is the lower limit of the summation. However, inasmuch as the number of zeros in $W_{kl}(r)$ increases with k, the first term of the series is also the largest, and we will use only this term for the present estimate.

Two laterally homogeneous Earth models are used in the computation, one characteristic of the Basin and Range mantle province (CITIII) after Archambeau, Flinn & Lambert (1969) and the other characteristic of an oceanic structure (Oceanic Series 304702). These models are described in Tables 1, 2 and Fig. 1. These elastic velocity–density models are representative of the extremes for the lateral structural variations in the Earth. Since the anelastic effects to be observed depend on the elastic velocity–density models, it is appropriate to consider velocity–density models other than a mean Earth model and to use the variation of predicted results between the models as a measure of the expected variations in the anelastic effects between different sampled regions. Since the models differ mainly in the upper mantle and in the crust, and are essentially the same below a depth of about 500 km, the effects on high-frequency oscillations will be most different between the models while the effects on the low frequency oscillations will nearly be the same. Further, the anelastic properties are expected to vary from region to region as well. We will, therefore,

Table 1

CITIII Basin and Range earth elastic model

	R	ρ	V_p	V_s	g
1	0.0	1.26200E 01	1.16375E 01	0.0	0.0
2	4.80000E 02	1.25630E 01	1.16375E 01	0.0	1.78319E 02
3	8.00000E 02	1.25123E 01	1.16375E 01	0.0	2.86197E 02
4	1.07849E 03	1.24202E 01	1.16375E 01	0.0	3.80575E 02
5	1.07849E 03	1.24202E 01	1.10900E 01	0.0	3.80575E 02
6	1.18286E 03	1.23740E 01	1.09300E 01	0.0	4.15572E 02
7	1.30115E 03	1.23151E 01	1.01100E 01	0.0	4.55081E 02
8	1.60202E 03	1.21415E 01	9.95904E 00	0.0	5.54626E 02
9	1.92202E 03	1.19115E 01	9.74884E 00	0.0	6.57413E 02
10	2.24202E 03	1.16353E 01	9.48778E 00	0.0	7.56068E 02
11	2.56202E 03	1.13001E 01	9.16066E 00	0.0	8.49804E 02
12	2.88202E 03	1.09183E 01	8.76934E 00	0.0	9.37662E 02
13	3.20202E 03	1.04731E 01	8.35837E 00	0.0	1.01870E 03
14	3.47900E 03	1.00500E 01	8.04000E 00	0.0	1.08254E 03
15	3.47900E 03	5.51000E 00	1.36710E 01	7.30000E 00	1.08254E 03
16	3.65643E 03	5.41659E 00	1.36182E 01	7.26856E 00	1.05738E 03
17	3.89643E 03	5.29729E 00	1.33198E 01	7.15484E 00	1.03238E 03
18	4.13643E 03	5.17729E 00	1.30254E 01	7.03751E 00	1.01539E 03
19	4.57100E 03	4.94961E 00	1.25500E 01	6.84800E 00	9.98546E 02
20	4.77100E 03	4.84782E 00	1.23300E 01	6.76000E 00	9.95811E 02
21	4.87100E 03	4.79622E 00	1.22100E 01	6.71700E 00	9.94781E 02
22	4.97100E 03	4.74050E 00	1.20800E 01	6.66700E 00	9.94340E 02
23	5.07100E 03	4.68451E 00	1.19400E 01	6.62100E 00	9.94250E 02
24	5.17100E 03	4.62992E 00	1.18000E 01	6.55400E 00	9.94426E 02
25	5.27100E 03	4.57531E 00	1.16800E 01	6.49600E 00	9.94930E 02
26	5.31100E 03	4.55347E 00	1.16500E 01	6.48000E 00	9.95175E 02
27	5.31700E 03	4.55019E 00	1.12800E 01	6.27400E 00	9.95370E 02
28	5.39100E 03	4.50500E 00	1.12300E 01	6.24600E 00	9.95802E 02
29	5.43100E 03	4.48000E 00	1.12000E 01	6.22900E 00	9.96193E 02
30	5.47100E 03	4.45247E 00	1.11700E 01	6.22300E 00	9.96550E 02
31	5.49100E 03	4.43985E 00	1.11600E 01	6.21700E 00	9.96748E 02
32	5.51100E 03	4.42450E 00	1.11450E 01	6.20900E 00	9.96928E 02
33	5.53100E 03	4.40905E 00	1.11300E 01	6.20000E 00	9.97058E 02
34	5.57100E 03	4.37000E 00	1.10850E 01	6.17500E 00	9.97432E 02
35	5.59100E 03	4.34995E 00	1.10550E 01	6.14800E 00	9.97585E 02
36	5.61100E 03	4.33103E 00	1.10300E 01	6.13500E 00	9.97740E 02
37	5.63100E 03	4.31092E 00	1.10000E 01	6.11800E 00	9.97876E 02
38	5.65100E 03	4.29040E 00	1.09700E 01	6.09300E 00	9.97956E 02
39	5.67100E 03	4.26901E 00	1.09600E 01	6.08700E 00	9.98108E 02
40	5.69100E 03	4.24500E 00	1.09400E 01	6.06600E 00	9.98204E 02
41	5.71100E 03	4.22011E 00	1.09300E 01	6.06100E 00	9.98302E 02
42	5.72600E 03	4.19950E 00	1.04300E 01	5.77400E 00	9.98355E 38
43	5.74100E 03	4.17650E 00	1.00000E 01	5.53600E 00	9.98390E 02
44	5.77100E 03	4.13041E 00	9.95000E 00	5.50000E 00	9.98438E 02
45	5.82100E 03	4.04082E 00	9.90000E 00	5.46400E 00	9.98348E 02
46	5.87100E 03	3.93995E 00	9.85000E 00	5.41800E 00	9.97983E 02
47	5.92100E 03	3.81000E 00	9.80000E 00	5.37300E 00	9.97297E 02
48	5.97100E 03	3.68195E 00	9.75000E 00	5.32900E 00	9.96240E 02
49	5.97300E 03	3.67750E 00	9.10000E 00	4.97400E 00	9.96200E 02
50	5.99600E 03	3.63427E 00	8.73000E 00	4.76400E 00	9.95578E 02
51	6.02100E 03	3.59401E 00	8.63000E 00	4.70200E 00	9.94887E 02
52	6.07100E 03	3.53000E 00	8.53000E 00	4.63900E 00	9.93351E 02
53	6.12100E 03	3.48258E 00	8.43500E 00	4.56400E 00	9.91757E 02
54	6.17100E 03	3.45000E 00	8.36000E 00	4.46900E 00	9.90156E 02
55	6.19100E 03	3.44030E 00	8.34000E 00	4.43400E 00	9.89518E 02
56	6.20100E 03	3.43750E 00	8.33500E 00	4.43200E 00	9.89225E 02
57	6.22500E 03	3.43430E 00	8.32500E 00	4.41800E 00	9.88505E 02
58	6.22500E 03	3.43400E 00	7.90000E 00	4.19200E 00	9.88505E 02
59	6.23100E 03	3.43350E 00	7.80000E 00	4.13600E 00	9.88370E 38
60	6.24100E 03	3.43127E 00	7.74000E 00	4.10800E 00	9.88097E 02
61	6.25100E 03	3.43079E 00	7.72500E 00	4.10700E 00	9.87736E 02
62	6.28100E 03	3.42994E 00	7.71900E 00	4.14000E 00	9.86918E 02
63	6.29100E 03	3.42994E 00	7.71500E 00	4.18100E 00	9.86652E 02
64	6.31100E 03	3.43026E 00	7.71500E 00	4.28500E 00	9.86112E 02
65	6.32600E 03	3.43028E 00	7.71900E 00	4.33300E 00	9.85725E 02
66	6.34300E 03	3.42810E 00	7.72000E 00	4.35900E 00	9.85310E 02
67	6.34300E 03	3.42810E 00	6.76000E 00	3.76300E 00	9.85310E 02
68	6.35700E 03	3.42799E 00	6.60000E 00	3.73700E 00	9.85012E 02
69	6.35700E 03	3.42799E 00	6.20000E 00	3.51100E 00	9.85012E 02
70	6.37100E 03	3.42756E 00	6.00000E 00	3.40700E 00	9.84836E 02

Table 2

Oceanic earth elastic model

	R	ρ	V_p	V_s	g
1	0.0	1.26200E 01	1.16375E 01	0.0	0.0
2	4.80000E 02	1.25830E 01	1.16375E 01	0.0	1.78319E 02
3	8.00000E 02	1.25123E 01	1.16375E 01	0.0	2.86197E 02
4	1.07849E 03	1.24202E 01	1.16375E 01	0.0	3.80575E 02
5	1.07849E 03	1.24202E 01	1.10900E 01	0.0	3.80575E 02
6	1.18286E 03	1.23740E 01	1.09300E 01	0.0	4.15572E 02
7	1.30115E 03	1.23151E 01	1.01100E 01	0.0	4.55081E 02
8	1.60202E 03	1.21415E 01	9.95904E 00	0.0	5.54626E 02
9	1.92202E 03	1.19115E 01	9.74884E 00	0.0	6.57413E 02
10	2.24202E 03	1.16353E 01	9.48778E 00	0.0	7.56068E 02
11	2.56202E 03	1.13001E 01	9.16066E 00	0.0	8.49804E 02
12	2.88202E 03	1.09183E 01	8.76934E 00	0.0	9.37662E 02
13	3.20202E 03	1.04731E 01	8.35837E 00	0.0	1.01870E 03
14	3.47900E 03	1.00500E 01	8.04000E 00	0.0	1.08254E 03
15	3.47900E 03	5.51000E 00	1.36710E 01	7.30000E 00	1.08254E 03
16	3.65643E 03	5.41659E 00	1.36182E 01	7.26856E 00	1.05738E 03
17	3.89643E 03	5.29729E 00	1.33198E 01	7.15484E 00	1.03238E 03
18	4.13643E 03	5.17729E 00	1.30254E 01	7.03751E 00	1.01539E 03
19	4.37643E 03	5.05696E 00	1.27788E 01	6.92733E 00	1.00446E 03
20	4.61643E 03	4.92649E 00	1.25211E 01	6.80733E 00	9.97982E 02
21	4.85643E 03	4.80434E 00	1.22317E 01	6.68447E 00	9.94891E 02
22	5.09643E 03	4.67062E 00	1.18912E 01	6.54580E 00	9.94251E 02
23	5.33643E 03	4.53958E 00	1.15279E 01	6.38712E 00	9.95346E 02
24	5.54050E 03	4.40006E 00	1.12034E 01	6.17887E 00	9.97138E 02
25	5.65224E 03	4.29022E 00	1.10055E 01	5.97256E 00	9.98000E 02
26	5.72100E 03	4.20539E 00	1.09000E 01	5.80711E 00	9.98340E 02
27	5.72100E 03	4.20539E 00	1.02600E 01	5.80711E 00	9.98340E 02
28	5.76100E 03	4.14600E 00	9.99000E 00	5.69142E 00	9.98427E 02
29	5.80100E 03	4.07896E 00	9.88667E 00	5.56000E 00	9.98398E 02
30	5.84100E 03	4.00324E 00	9.79667E 00	5.41502E 00	9.98225E 02
31	5.88100E 03	3.91575E 00	9.72000E 00	5.26184E 00	9.97876E 02
32	5.91100E 03	3.83880E 00	9.65500E 00	5.14681E 00	9.97471E 02
33	5.94100E 03	3.75850E 00	9.56000E 00	5.03233E 00	9.96926E 02
34	5.95600E 03	3.71866E 00	9.46000E 00	4.97582E 00	9.96598E 02
35	5.97600E 03	3.67034E 00	9.46000E 00	4.90171E 00	9.96110E 02
36	5.97600E 03	3.67034E 00	9.06700E 00	4.90171E 00	9.96110E 02
37	5.98600E 03	3.65190E 00	8.80000E 00	4.86542E 00	9.95848E 02
38	5.99600E 03	3.63427E 00	8.78000E 00	4.82955E 00	9.95578E 02
39	6.00600E 03	3.61766E 00	8.73000E 00	4.79413E 00	9.95300E 02
40	6.03100E 03	3.58003E 00	8.63500E 00	4.70807E 00	9.94575E 02
41	6.07100E 03	3.53000E 00	8.54821E 00	4.58000E 00	9.93351E 02
42	6.08400E 03	3.51615E 00	8.52000E 00	4.54172E 00	9.92941E 02
43	6.10100E 03	3.49668E 00	8.46300E 00	4.49469E 00	9.92398E 02
44	6.12100E 03	3.48258E 00	8.42000E 00	4.44453E 00	9.91757E 02
45	6.14100E 03	3.46783E 00	8.36700E 00	4.40088E 00	9.91114E 02
46	6.17100E 03	3.45000E 00	8.32010E 00	4.35000E 00	9.90156E 02
47	6.17100E 02	3.45000E 00	7.70000E 00	4.35000E 00	9.90156E 02
48	6.22100E 03	3.43442E 00	7.70000E 00	4.31394E 00	9.88613E 02
49	6.25100E 03	3.43079E 00	7.70000E 00	4.33003E 00	9.87736E 02
50	6.27600E 03	3.42994E 00	7.70000E 00	4.37016E 00	9.87041E 02
51	6.28600E 03	3.42994E 00	7.70000E 00	4.39388E 00	9.86774E 02
52	6.31450E 03	3.43026E 00	7.70000E 00	4.48852E 00	9.86043E 02
53	6.32300E 03	3.43028E 00	7.70010E 00	4.52514E 00	9.85834E 02
54	6.32300E 03	3.43028E 00	8.20100E 00	4.52514E 00	9.85834E 02
55	6.36300E 03	3.42799E 00	8.20010E 00	4.75618E 00	9.84903E 02
56	6.36400E 03	3.42785E 00	8.20010E 00	4.76330E 00	9.84880E 02
57	6.36400E 03	3.42785E 00	6.41000E 00	4.76330E 00	9.84880E 02
58	6.36600E 03	3.42756E 00	6.41000E 00	4.77774E 00	9.84836E 02
59	6.36600E 03	1.03000E 00	1.51000E 00	0.0	9.84836E 02
60	6.37100E 03	1.03000E 00	1.51000E 00	0.0	9.84836E 02

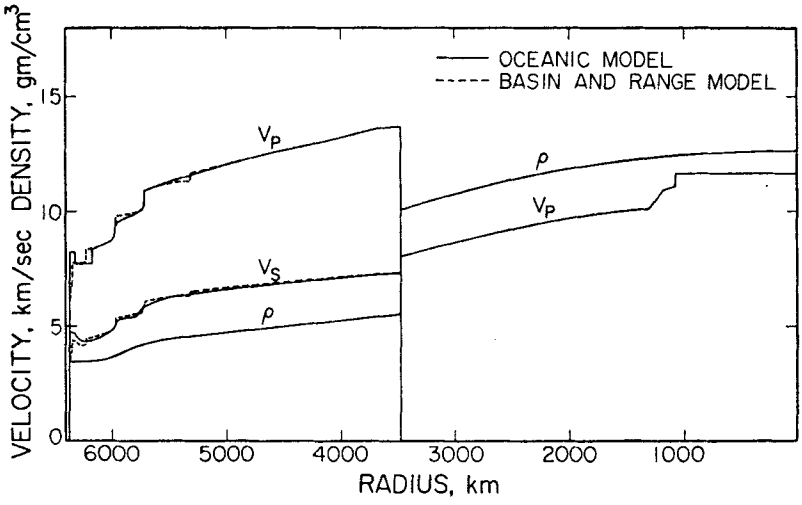

FIG. 1. Laterally homogeneous earth elastic models used in the perturbation calculations.

employ a number of different anelastic models in combination with the two elastic models in order to estimate the total variability of the anelastic perturbation effects.

Five intrinsic Q models are employed for the Basin and Range Earth model. Two of them are frequency independent with their low Q zone corresponding to the low velocity channel of the Earth. The only difference between these two Q models, $Q(H_1)$ and $Q(L_1)$, is in their numerical values inside the low Q zone. This type of frequency-independent Q-model was adopted in the early work to construct intrinsic Q-models in the Earth's interior (Anderson & Archambeau 1964). The next two

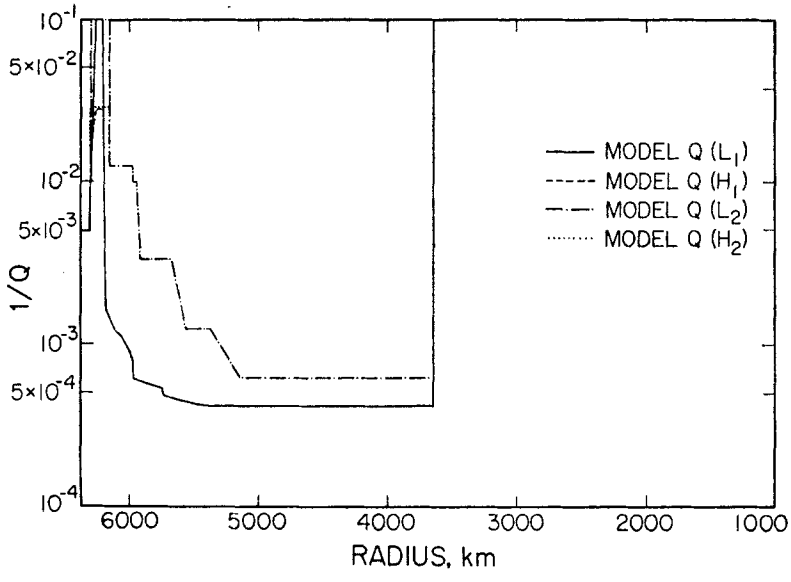

FIG. 2. Frequency-independent earth intrinsic Q models used in the perturbation calculations. Numerical values of these Q models are listed in Tables 3 and 4.

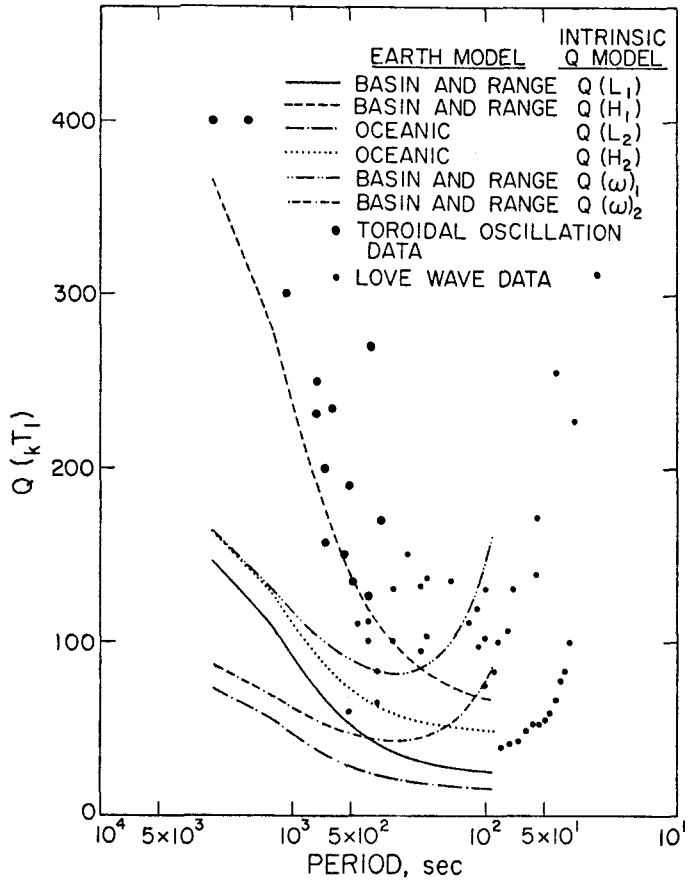

FIG. 3. Free oscillation quality factor (fundamental toroidal modes) calculated from various earth elastic and intrinsic Q models as compared with the observational data. The observational data are from Gutenberg (1924), Wilson (1940), Sato (1958), Alsop *et al.* (1961), Press *et al.* (1961), MacDonald & Ness (1961), Smith (1961), Båth & Lopez-Arroyo (1962), Nowroozi (1968) and Solomon (1972).

intrinsic Q models, $Q(\omega)_1$ and $Q(\omega)_2$ are based on a single relaxation mechanism for seismic energy dissipation. They are frequency dependent and, except for a scaling factor, are after Jackson's model 10–04 (Jackson 1969). The last intrinsic Q-model for Basin and Range Earth model $Q(\omega)_3$, is constructed after Solomon (1972). In this model, the Q is independent of frequency above the low velocity zone and is the result of two relaxation mechanisms (one of which is attributed to partial melting) in the low velocity zone. This model is frequency dependent through only one relaxation mechanism below the low velocity zone and above the core–mantle boundary. Only frequency independent Q models, $Q(L_2)$ and $Q(H_2)$, are employed for the oceanic Earth model. The Basin and Range Q-models are listed in Table 3. The oceanic Q-models are listed in Table 4. The frequency independent Q-models are also shown in Fig. 2.

The computed free oscillation quality factor $Q_{k=0,\,l}$ for various Earth models and for various intrinsic Q-models is plotted in Figs 3 and 4. The attenuation data for free oscillations and surface waves up to 1970 have been collected by Jackson & Anderson (1970). The toroidal oscillation and Love-wave attenuation data reproduced in Figs 3 and 4 with the various computed $Q_{k=0,\,l}$ are from this collection

Table 3

Basin and Range intrinsic Q models

Depth, z (km)	$Q(L_1)$	$Q(H_1)$	$Q(\omega)_1$	$Q(\omega)_2$	$Q(\omega)_3$
0–28	200	200	$Q^{-1}(\omega) \equiv Q^{-1}(\omega; A, \tau_0, E^*, V^*)$		1000
28–45	120	130	$= A\,\omega\tau/(1+\omega^2\tau^2)$		$Q^{-1} = 0{\cdot}1\,[\omega\tau_1/(1+\omega^2\tau_1^2)$
45–60	35	55	$\tau = \tau_0 \exp[(E^*+PV^*)/RT]$		$+\omega\tau_2/(1+\omega^2\tau_2^2)]$
60–80	20	43	$\tau = 0{\cdot}4$ sec		$\tau_2 = 4\times10^{-4}\tau_1$†
80–140	10	36	$E^* = 10$ kcal/mole		$Q^{-1} = 0{\cdot}1\,\omega\tau_3/(1+\omega^2\tau_3^2)$
140–146	15	38	$V^* = 4$ cm^3/mole		
146–170	315	325			
170–180	615	615	Pressure Model: Bullen Model B		$\tau_3 = 2$ sec
180–200	655	655	(Bullen 1965)		
200–250	755	755	Temperature Model: MacDonald		
250–300	860	860	Model 19 (MacDonald 1959)		
300–350	965	965			
350–375	1078	1078			
375–398	1190	1190			
398–400	1443	1443			
400–450	1645	1645			
450–500	1695	1695			
500–550	1745	1745	$A = 0{\cdot}032$	$A = 0{\cdot}060$	
550–600	1795	1795			
600–630	1835	1835			
630–645	1858	1858			
645–660	1973	1973			
660–680	2090	2090			
680–700	2110	2110			
700–720	2130	2130			
720–740	2150	2150			
740–760	2170	2170			
760–780	2190	2190			
780–800	2210	2210			
800–840	2240	2240			
840–860	2270	2270			
860–880	2290	2290			
880–900	2310	2310			
900–940	2340	2340			
940–980	2370	2370			
980–1054	2390	2390			
1054–2892	2400	2400			
2892–6371	0	0			

† $\tau_1 = 20 \exp[-(500\,E^*+584\,V^*)/1239+(500\,E^*+4\,zV^*)/T]$ sec; $E^* = 57$ kcal/mole, $V^* = 1{\cdot}0$ cm^3/mole; Temperature Model 200029 after Minster & Archambeau (1971).

Table 4

Oceanic frequency-independent intrinsic Q models

Depth (km)	$Q(L_2)$	$Q(H_2)$
0–5	0	0
5–48	200	200
48–200	10	35
200–395	80	80
395–446	100	100
446–825	300	300
825–1155	800	800
1155–2892	1600	1600
2892–6371	0	0

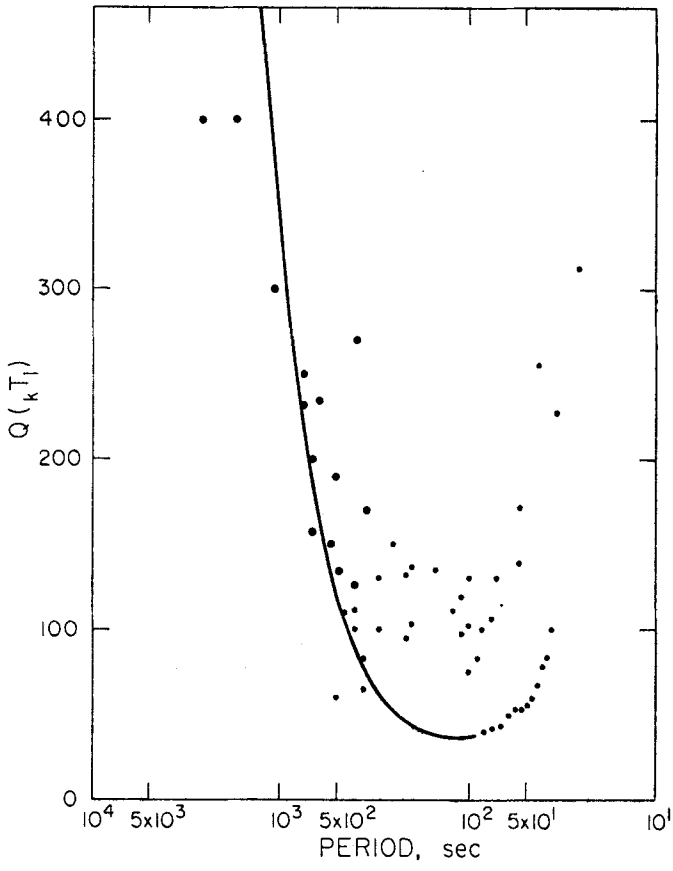

FIG. 4. Free oscillation quality factor (fundamental toroidal modes) calculated from Earth Basin and Range elastic model and the frequency-dependent intrinsic Q model, $Q(\omega)_3$, as compared with the same observational data as those in Fig. 3. The fit is much better than those in Fig. 3.

except for the 12 points at the lower right corner, which are from Solomon (1972). The attenuation data included in Figs 3 and 4 are from Nowroozi (1968; ${}_0T_l$), Alsop, Sutton & Ewing (1961; ${}_0T_l$), MacDonald & Ness (1961; ${}_0T_l$), Smith (1961; ${}_0T_l$), Solomon (1972; Love wave), Savarenskii, Nersesov & Karmaleeva (1966; Love wave), Bath & Lopez-Arroyo (1962; Love wave), Press, Ben-Menahem & Toksöz (1961; Love wave), Satô (1958; Love wave), Wilson (1940; Love wave), Gutenberg (1924; Love wave). It appears that the intrinsic Q-models $Q(H_1)$, $Q(H_2)$ and $Q(\omega)_1$ give seismic attenuation which agrees well with the observed data. However, noting the wide scatter of seismic attenuation data and some recent results of surface wave attenuation in the western United States (Solomon 1972), the low $Q_{k=0,\,l}$ values produced by the intrinsic Q-models, $Q(L_1)$, $Q(L_2)$ and $Q(\omega)_2$, cannot be ruled out as unreasonable. Values of $Q_{k=0,\,l}$ calculated from $Q(\omega)_3$, the most sophisticated among the Q-models, matches both the long period free oscillation attenuation data and short-period Love-wave attenuation data in the western United States. Shifts in free oscillation periods calculated from this intrinsic Q-model, $Q(\omega)_3$, are taken to be representative. The period shift

$$|_{i=1}(DT)_{k=0,\,l}| = T_{k=0,\,l}\left|\frac{{}_{i=1}\omega^{(2)}_{k=0,l}}{\omega_{k=0,\,l}}\right| = T_{k=0,\,l}\left\{\frac{{}_{i=1}\gamma^{(2)}_{k=0,l}}{2} + \frac{1}{2}\left(\frac{\gamma^{(1)}_{k=0,l}}{2}\right)^2\right\} \qquad (37)$$

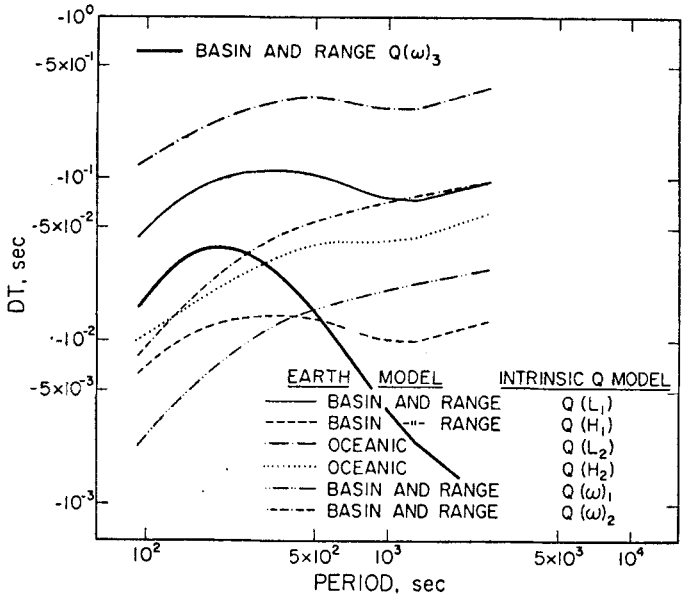

FIG. 5. Shift in fundamental toroidal free oscillation periods, DT, due to anelasticity as calculated from various earth elastic and intrinsic Q models.

and the fractional period shift, $|_{i=1}(DT)_{k=0,\,l}/T_{k=0,\,l}|$, as calculated from various Earth and intrinsic Q-models are plotted in Figs 5 and 6. The maximum values of $|DT/T|$ and the modes at which they occur are listed in Table 5 for various Earth and intrinsic Q models. When appropriate ($l \gg 1$), the shift in free oscillation period is also expressed as the shift in phase and group velocities of surface waves (Press 1964). The phase and group velocities of the two Earth models are plotted in Fig. 7. The shift in phase and group velocities for various Earth and intrinsic Q-models are plotted in Figs 8 and 9.

Table 5

Maximum percentage shift of toroidal free oscillation period calculated from various earth elastic and intrinsic Q models

Earth elastic model	Earth intrinsic Q model	Free oscillation mode at which maximum occurs	Calculated free oscillation period (s)	Maximum value of shift ($\times 10^{-2}$)
Oceanic	$Q(L_2)$	${}_0T_{92}$	92·89	−13·104
Oceanic	$Q(H_2)$	${}_0T_{99}$	86·63	−1·0936
Basin & Range	$Q(L_1)$	${}_0T_{62}$	140·43	−5·4140
Basin & Range	$Q(H_1)$	${}_0T_{68}$	129·29	−0·7396
Basin & Range	$Q(\omega)_1$	$0T_{30}$	261·68	−0·3815
Basin & Range	$Q(\omega)_2$	${}_0T_{30}$	261·68	−1·3412
Basin & Range	$Q(\omega)_3$	${}_0T_{60}$	144·59	−2·3022

4. Discussion

The range of toroidal oscillations for which the maximum fractional period shift occurs depends on the Earth elastic and intrinsic Q-structure model, but in general it is controlled by the low velocity zone where anelastic behaviour is an outstanding feature. This is apparent in Table 5, where the longest period (calculated from various Earth elastic and intrinsic Q-models) at which the maximum fractional shift occurs is 261·68 s. The period at which the maximum fractional shift occurs is 144·59 s for the most representative Q-model, $Q(\omega)_3$. For the longer period free oscillations of ${}_0T_l$, most of the energy is distributed outside of the low velocity zone. For much shorter period free oscillations ${}_0T_l$, the displacement field does not sample much of the low velocity zone, hence the peaked influence of anelasticity.

The maximum fractional shift in Table 5 is $-1{\cdot}31\times10^{-3}$ for an Oceanic Earth model with a more extreme intrinsic Q distribution given by model $Q(L_1)$. The maximum fractional shift for the more representative intrinsic Q structure, $Q(\omega)_3$, on a Basin and Range Earth model is $-2{\cdot}30\times10^{-4}$. Expressed in a different way, we see from Figs 8 and 9 that the shifts in phase and group velocities (e.g. the anelasticity induced dispersion of surface waves) are of the order of 0·007 km s^{-1} for the Oceanic model $Q(L_2)$ and at most 0·001 km s^{-1} for the Basin and Range Q-model $Q(\omega)_3$. The largest effects occurring at around 150-s period for both models.

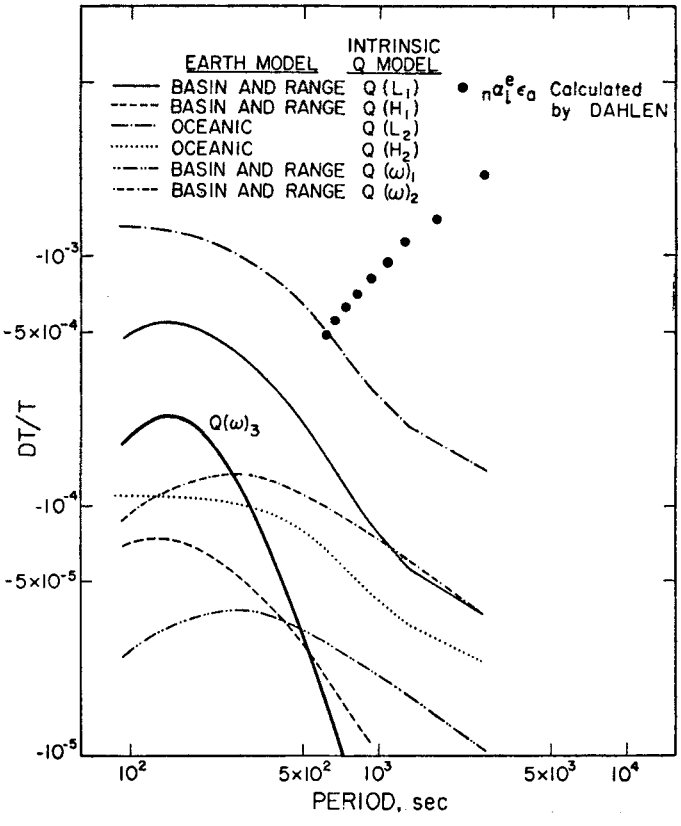

FIG. 6. Fractional shift in fundamental toroidal free oscillation periods, DT/T, due to anelasticity as calculated from various earth elastic and intrinsic Q models. The values ${}_n\alpha_l{}^e\varepsilon_a$ calculated by Dahlen (1968) are the fractional shift of toroidal oscillation periods due to ellipticity alone.

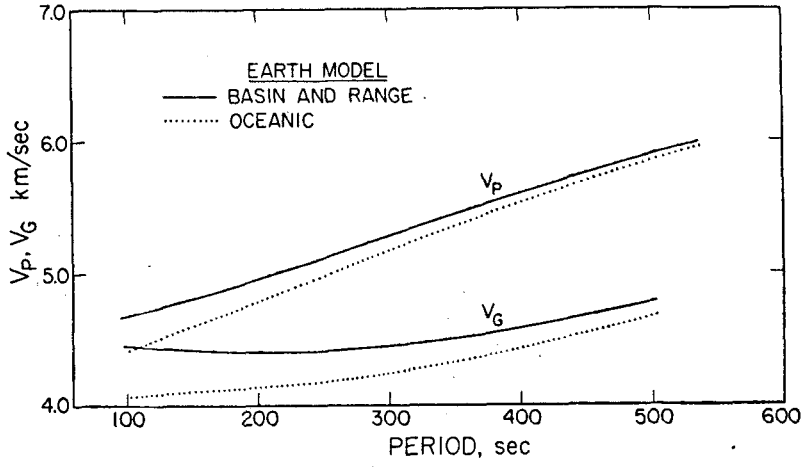

FIG. 7. Love wave phase velocity, V_P, and group velocity V_G, as calculated from the two earth elastic models used in the perturbation calculations.

As previously noted, the resolution of the fundamental toroidal modes ${}_0T_l$ reported by Dziewonski & Gilbert (1972) varies between 0·031 and 0·262 per cent and is generally about 0·1 per cent for the higher frequency toroidal modes ${}_0T_l$, where the anelastic shift becomes important. This kind of resolution, although comparable to the maximum fractional period shift produced by the more extreme Q-model, $Q(L_1)$, is generally five times larger than the maximum fractional period shift produced by the more representative Q-model $Q(\omega)_3$. Therefore, the anelastic shifts are generally smaller than the observational uncertainties in the normal mode data. However, the free oscillation data are obtained by averaging individual observations. Since we find that the anelastic effects are largest in the surface-wave period range, it is more appropriate to compare the magnitude of the predicted effects to surface-wave dispersion data for surface waves propagating within particular tectonic

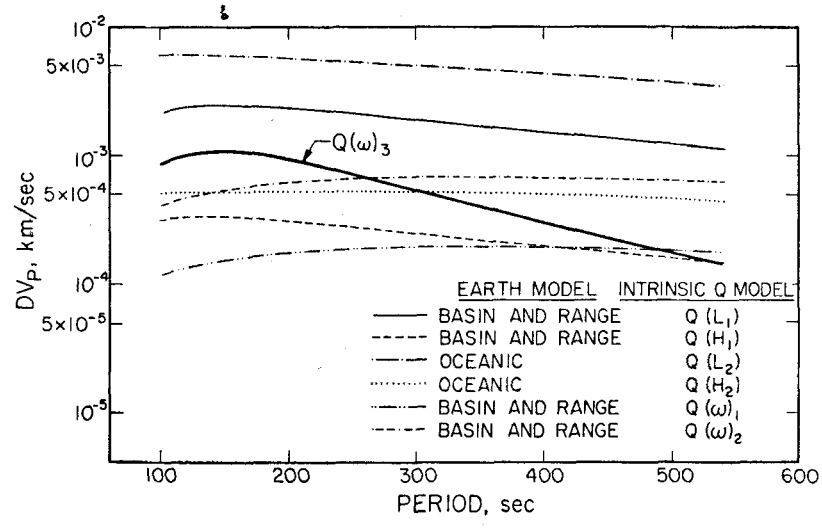

FIG. 8. Shift in Love wave phase velocity DV_P, due to anelasticity calculated from various earth elastic and intrinsic Q models.

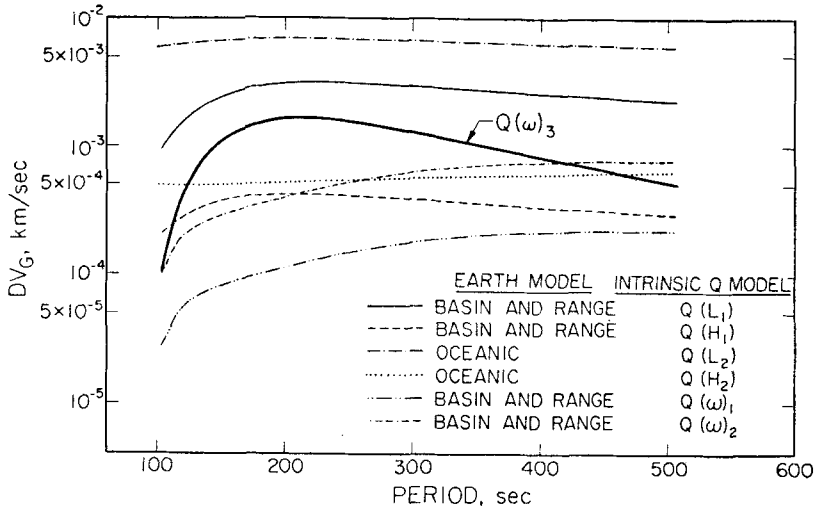

FIG. 9. Shift in Love wave group velocity, DV_G, due to anelasticity calculated from various earth elastic and intrinsic Q models.

provinces rather than to data expressed as an average from measurements obtained from many locations scattered on the Earth's surface. We observe for this comparison that the dispersive effects of anelasticity for periods greater than 100-s result in a more or less uniform shift in the group and phase velocities of about 0·005 km s^{-1}, although shifts of the order of 0·01 km s^{-1} or greater can be expected for a very low Q upper mantle model. Effects of this magnitude are at the threshold of resolution with current methods of measurement. If 'pure path' surface-wave data within a low Q region are available such that the anelastic effects are large and lateral variation in the velocity-density structure over the path minimal, then it is likely that the dispersive effects of anelasticity will be resolvable and that a joint inversion for elastic and anelastic properties will be a useful approach. However, it is clear that the anelastic attenuation, involving the spectral amplitude decrement, will dominate the inversion for the anelastic properties of the medium with the observed dispersion being most important in determining the elastic properties and only weakly constraining the inversion for the anelastic structure.

Fig. 10 is an example of some high resolution surface-wave dispersion data that are required in the joint inversion for elastic and anelastic properties of the medium. For such dispersion data, extended on to around 200 s, it is reasonable to expect that the data uncertainties will be small enough to provide a constraint on the anelastic properties, provided that high resolution filtering techniques are used.

It is important to ask how does the period shifts due to anelasticity compare with the effects of ellipticity, rotation, and lateral heterogeneity. Dahlen (1968) calculated values up to ${}_0T_{10}$ for ellipticity and rotational effects. The fractional shifts in period of the central line of the multiplet ($m = 0$) due to ellipticity alone ${}_n\alpha_l^e \varepsilon_a$, as calculated by Dahlen are plotted in Fig. 6, together with fractional shifts caused by anelasticity. The trend shows that at modes where anelasticity effects are important, namely in the period range 50–300 s, the effect of ellipticity alone on the shift in period of the central line of the multiplet ($m = 0$) is less than the anelastic effects. For orders $l < 10$, ellipticity is the dominant effect. The rotational effect, considered alone, does not produce any period shift in the central line ($m = 0$). When rotation and ellipticity are considered together, the perturbation effects are coupled (Dahlen 1968, 1969).

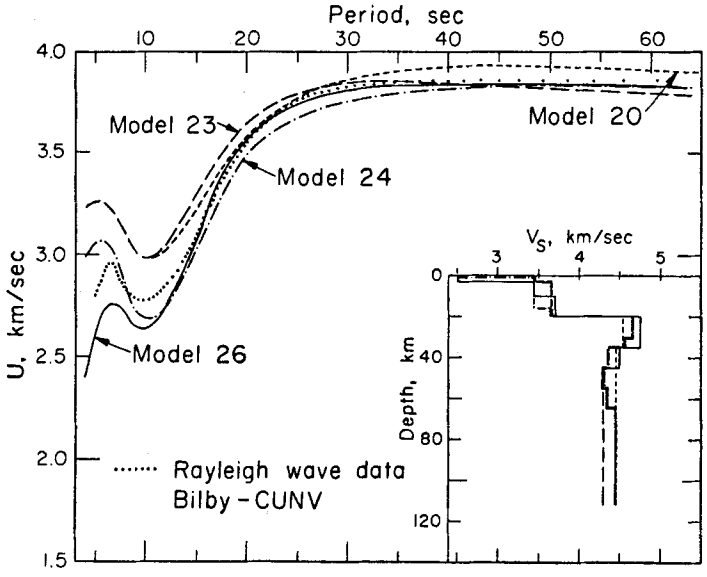

FIG. 10. Observed group velocity dispersion for Rayleigh wave propagation within the Basin and Range province. The dots are individual, independent determinations of the group velocity at particular frequencies obtained by narrow band filtering methods. In this exceptional case, the relative resolution is estimated to be of the order of 0·001 km s^{-1}. The other curves are theoretical dispersion curves corresponding to the velocity structures shown in the inset. (From Davies, Archambeau & Wu, private communication).

However, the overall effects of ellipticity and rotation are still characterized by perturbations that are strongest in the range of order number l less than 30. For higher orders, anelastic effects are larger. Luh (1973) calculated the combined perturbation effects of rotation, ellipticity and the lateral inhomogeneity due to difference in crust–mantle structure between continents and oceans. As would be expected, the effect of the strong continental-oceanic structure variation gives rise to a significant effect at nearly all order numbers. In the period range where anelasticity is important, effects of lateral structural variations on the periods can be much larger than all other perturbations including anelasticity if the free oscillation data are averaged globally. However, since the free oscillation data are more meaningfully viewed in terms of surface waves in the 50- to 300-s period range, the importance of lateral structure variations are dependent on the lateral inhomogeneity of the region sampled by the surface waves. Therefore, for selectively sampled surface-wave paths, effects of lateral inhomogeneity can be minimized and it is likely that the anelastic effects will predominate as the important deviation from an ideal elastic, radially inhomogeneous Earth model. This appears to be the case for the data shown in Fig 10, for example. We note also that the lateral inhomogeneity in the anelastic properties will affect the frequency splitting pattern of the free oscillation spectra as calculated from Luh's model (1973).

The numerical calculation of the present study is carried out only for toroidal oscillations of the Earth since the anelastic effect is more pronounced for toroidal modes than for spheroidal modes. This is because toroidal oscillations involve shear motion only, for which seismic dissipation is most effective. However, Dziewonski & Gilbert (1972) reported that the observational accuracy of spheroidal free oscillation periods are generally two orders of magnitude higher than those of the toroidal modes.

This can be understood at least partially from the fact that spheroidal modes have a higher quality factor than the toroidal modes. Because of the greater accuracy of measurement, it may be useful to calculate the shifts in free oscillation periods for spheroidal modes, which probably have the same relative importance as for the toroidal free oscillations. The spheroidal oscillation amplitude decrement and period data could also be used to determine the Earth's anelastic properties.

Acknowledgments

This work was supported by American Petroleum Institute under API Research Project IV. The authors wish to thank Dr Thomas Jordan who provided the computer program for the calculation of the displacement field and angular frequency of the Earth's toroidal oscillations.

Hsi-Ping Liu:
Seismological Laboratory,
Division of Geological and Planetary Sciences,
California Institute of Technology,
Pasadena, California 91125.

Charles B. Archambeau:
CIRES,
University of Colorado,
Boulder, Colorado 80302.

References

Alsop, L. E., Sutton, G. H. & Ewing, M., 1961. Measurement of Q for very long period free oscillations, *J. geophys. Res.*, **66,** 2911–2915.

Alterman, Z., Jarosch, H. & Pekeris, C. L., 1959. Oscillations of the earth, *Proc. R. Soc.*, **A252,** 80–95.

Anderson, D. L. & Archambeau, C. B., 1964. The anelasticity of the earth, *J. geophys. Res.*, **69,** 2071–2084.

Archambeau, C. B., Flinn, E. A. & Lambert, D. G., 1969. Fine structure of the upper mantle, *J. geophys. Res.*, **74,** 5825–5865.

Backus, G. E., 1967. Converting vector and tensor equations to scalar equations in spherical coordinates, *Geophys. J. R. astr. Soc.*, **13,** 71–101.

Bath, M. & Lopez-Arroyo, A., 1962. Attenuation and dispersion of G waves, *J. geophys. Res.*, **67,** 1933–1942.

Bullen, K. E., 1965. *An introduction to the theory of seismology*, 3rd edition, Cambridge University Press, Cambridge, p. 238.

Dahlen, F. A., 1968. The normal modes of a rotating elliptical earth, *Geophys. J. R. astr. Soc.*, **16,** 329–367.

Dahlen, F. A., 1969. The normal modes of a rotating, elliptical Earth—II: Near-resonance multiplet coupling, *Geophys. J. R. astr. Soc.*, **18,** 397–436.

Dziewonski, A. M. & Gilbert, F., 1972. Observation of normal modes from 84 record of the Alaskan earthquake of 1964 March 28, *Geophys. J. R. astr. Soc.*, **27,** 393–446.

Gordon, R. B. & Nelson, C. W., 1966. Anelastic properties of the earth, *Rev. Geophys.*, **4,** 457–474.

Gutenberg, B., 1924. Dispersion und extinktion von seismischen Oberflachenwellen und der Aufbau der obersten Erdschichten, *Physik. Z,* **25,** 377–381.

Jackson, D. D., 1969. Elastic relaxation model for seismic wave attenuation in the earth, *Phys. Earth Planet. Int.*, **2**, 30–34.

Jackson, D. D. & Anderson, D. L., 1970. Physical mechanisms of seismic-wave attenuation, *Rev. Geophys. Space Phys.*, **8**, 1–63.

Luh, P. C. H., 1973. *The normal modes of the rotating, self-gravitating, inhomogeneous earth*, PhD thesis, University of California, San Diego.

MacDonald, G. J. F., 1959. Calculations on the thermal history of the earth, *J. geophys. Res.*, **64**, 1967–2000.

MacDonald, G. J. F. & Ness, N. F., 1961. A study of the free oscillations of the earth, *J. geophys. Res.*, **66**, 1865–1912.

Minster, J. B. & Archambeau, C. B., 1971. Thermal models of the earth, paper presented at *Heat Flow Symposium of I.U.G.G.*, Moscow, USSR.

Nowroozi, A. A., 1968. Measurements of Q values from the free oscillations of the Earth, *J. geophys. Res.*, **73**, 1407–1415.

Press, F., 1964. Long-period waves and free oscillations of the earth, in *Research in Geophysics*, vol. 2, The MIT Press, Cambridge, pp. 1–26.

Press, F., Ben-Menaham, A. & Toksöz, M. N., 1961. Experimental determination of earthquake fault length and rupture velocity, *J. geophys. Res.*, **66**, 3471–3485.

Sato, Y., 1958. Attenuation, dispersion, and the waveguide of the G waves, *Bull. seism. Soc. Am.*, **48**, 231–251.

Savarenskii, E. F., Nersesov, I. L. & Karmaleeva, R. M., 1966. Observations of long period waves of the Aleutian earthquake of 4 February 1965 recorded by quartz extensometers, *Izv. Earth Phys.*, **5**, 33–42 (translation).

Smith, S. W., 1961. *An investigation of the earth's free oscillation*, PhD thesis, California Institute of Technology.

Solomon, S. C., 1972. Seismic-wave attenuation and partial melting in the upper mantle of North America, *J. geophys. Res.*, **77**, 1483–1502.

Wilson, J. T., 1940. The Love waves of the fourth Atlantic earthquake of August 28, 1933, *Bull. seism. Soc. Am.*, **30**, 273–301.